Structural Control & Health Monitoring
The Journal of the International Association for Structural Control and Monitoring

Vibration control of spar-type floating offshore wind turbine towers using a tuned mass-damper-inerter

Journal:	*Structural Control and Health Monitoring*
Manuscript ID	STC-19-0130.R1
Wiley - Manuscript type:	Research Article
Date Submitted by the Author:	n/a
Complete List of Authors:	Sarkar, Saptarshi; University of Dublin Trinity College, Civil, Structural and Environmental Engineering Fitzgerald, Breiffni; University of Dublin Trinity College, Civil, Structural and Environmental Engineering
Keywords:	offshore wind turbine, vibration control, TMD, TMDI, Inerter, Stochastic wind-wave loads

Received: Added at production | Revised: Added at production | Accepted: Added at production

DOI: xxx/xxxx

RESEARCH ARTICLE

Vibration control of spar-type floating offshore wind turbine towers using a tuned mass-damper-inerter

Saptarshi Sarkar | Breiffni Fitzgerald*

[1]Department of Civil, Structural and Environmental Engineering, Trinity College Dublin, Dublin, Ireland

Correspondence
*Breiffni Fitzgerald, Department of Civil, Structural and Environmental Engineering, Trinity College Dublin, Ireland. Email: breiffni.fitzgerald@tcd.ie

Summary

This paper investigates the use of a passive tuned mass-damper-inerter (TMDI) for vibration control of spar-type floating offshore wind turbine towers. The TMDI is a relatively new concept as a passive vibration control device. The configuration consists of an 'inerter' attached to the tuned mass, parallel to the spring and damper of a classical tuned mass damper (TMD). The inerter provides a mass amplification effect on the classical TMD. The presence of the inerter virtually increases the mass of the damper leading to greater vibration control capabilities. This enables one to achieve improved vibration control using a lighter damper. Using a lightweight damper is particularly important for an offshore wind turbine since increasing mass on top of the tower can destabilize the overall system and increase tower vibrations, as demonstrated in this paper. The development of a passive TMDI for an offshore wind turbine tower has been proposed in detail in this work. Numerical simulations have been performed and results are presented demonstrating the impressive vibration control capabilities of this new device under various stochastic wind-wave loads. It has been shown that the TMDI has considerable advantages over the classical TMD, achieving impressive response reductions with reductions in the stroke of the tuned mass. The TMDI has been shown to be a promising candidate for replacing the classical TMD for offshore wind applications.

KEYWORDS:
Offshore wind turbine, Vibration control, TMD, TMDI, Inerter, Stochastic wind-wave loads

1 | INTRODUCTION

Offshore wind turbines are the largest rotating structures on earth. Wind turbine towers are very flexible structures that must support a large mass at their tip. It is not uncommon for modern towers to exceed 120 m in height. These structures are subjected to turbulent aerodynamic loads and hydrodynamic loads and must remain operational in very harsh environments. Wind turbine towers are dynamically sensitive and as such tower vibrations can cause damage to acceleration sensitive equipment housed in the nacelle leading to malfunctions causing turbine shutdown and reduced power output. Dueñas-Osorio and Basu [1] demonstrated the unavailability of wind turbines due to tower vibrations. Much work has been undertaken in the past decade to control vibrations of wind turbine towers. Tower vibrations may have a significant impact on downtime, lifetime of the components, and even on the overall integrity of the structural system. These impacts will have associated implications for the cost of wind power.

Therefore, there is now increasing interest on reducing the harmful effects of mechanical vibration on wind turbine towers in the wind energy industry.

The application of structural control devices to wind turbines is now a very active area of research. Studies have been carried out to investigate the effectiveness of various devices such as Tuned Liquid Dampers[2,3]; Tuned Liquid Column Dampers[4]; Circular Liquid Dampers[5]; and Roller Dampers[6] when applied to wind turbines. Tuned Mass Dampers (TMDs) have been investigated in many studies. Murtagh et al.[7], Lackner and Rotea[8] and Fitzgerald et al.[9] demonstrated the effectiveness of passive tuned mass dampers (TMDs) in reducing blade vibration. Arrigan et al.[10] and Fitzgerald et al.[11] developed semi-active TMDs to control the vibrations of wind turbine towers and blades. Active TMDs have also been investigated by Lackner and Rotea[12], Fitzgerald and Basu[13], and Fitzgerald et al.[9,14]. Liquid dampers have also been used by researchers for vibration control of wind turbines. Tuned Liquid Column Damper (TLCD) was used by Colwell and Basu[4], Zhang et al.[2]; Tuned Liquid Damper (TLD) was used by Zhang et al.[3], Circular Liquid Column Damper was used by Basu et al.[5] and Magneto-Rheological Tuned Liquid Column Damper (MR-TLCD) were used by Sarkar and Chakraborty[15,16]. The industry has embraced this research and modern multi-megawatt wind turbines are now designed and deployed with TMDs at the top of their towers as standard (see[17] and[18]).

In the meantime there have been some important developments in relation to TMDs. Recent studies have shown that using so called 'inerters' in TMDs improves the effectiveness of these devices. Smith[19] presented the concept of the inerter. The ideal inerter was defined as "a mechanical two-node, one-port device with the property that the equal and opposite force applied at the nodes is proportional to the relative acceleration between the nodes". The constant of proportionality was termed the 'inertance' with units of kilogrammes. Smith stated that one possible application of the inerter would be that of mechanical vibration suppression. In recent years the inerter has been applied in the fields of vibration control and structural control, with many studies investigating novel TMD configurations incoporating inerters. TMD performance is heavily dependent on the mass ratio, however, inerter-based TMDs employ a 'gearing' that ensures the effective mass of the device is much greater than the actual mass of the device. The mass amplification is usually achieved via a rack and pinion mechanism or inertial hydraulic devices. Inerter-based TMDs can therefore achieve larger effective mass ratios than classical TMDs without excessive weight in the damper. Ikago et al.[20] developed a novel tuned viscous mass damper (TVMD) for seismic applications. This device utilises an inerter, in the form of a ball screw mechanism and spring connected to the primary structure, to provide an apparent mass amplification to the TMD. The authors derived a closed-form expression for optimum TVMD design and verified the efficacy of the device with shake table tests. Garrido et al.[21] devised a novel device they termed a rotational inertia double-tuned mass damper (RIDTMD). This device consists of a traditional TMD with the viscous damper element replaced with a TVDM. The authors derived optimum parameters for the RIDTMD. The RIDTMD was found to be more effective than a TMD of the same mass ratio with a broader suppression band and nearly identical stroke. Marian and Giaralis[22] utilised the inerter to develop a novel passive damper they have called the tuned mass-damper-inerter (TMDI). This device takes advantage of the mass amplification effect of the inerter to achieve improved performance over a classical TMD of the same mass ratio. Lazar et al.[23] also proposed a novel TMD device utilising the inerter. The new device uses the inerter's principle of mass amplification to improve on the performance of classical TMDs. Hu and Chen optimally designed inerter-based devices for random force excitation on the primary system using a numerical optimization method[24].

All of these studies have demonstrated that inerters are capable of producing a large effective mass by using a relatively small physical mass. TMDs equipped with inerters, TMDIs, therefore require a smaller physical mass than classical TMDs to be effective. Since the mass ratio, i.e. the ratio of the mass of the TMD to the mass of the primary structure, is the governing parameter that affects the performance of a TMD this is a significant development.

There have been some recent works on the use of inerter-based devices for vibration control of wind turbines. Hu et al.[25] applied an inerter-based structural control device to a barge-type floating offshore wind turbine. The inerter consisted of a parallel connection of a spring, a damper, and an inerter-based network. Zhang et al.[26] proposed the tuned parallel inerter mass system (TPIMS) for seismic response mitigation of wind turbine towers. Using the TPIMS the tower top displacement, base shear, and moment were reduced significantly compared to results with a classical TMD of the same mass ratio. Ma et al.[27] developed the tuned heave plate inerter (THPI), an inerter-based device for vibration control of semi submersible platform heave motions. The presence of the inerter transforms the linear motion into high-speed rotation thereby amplifying the damper mass. The THPI was shown to be more effective at controlling vibrations than conventional structural control schemes.

In this paper, a TMDI is employed to reduce tower vibrations in spar-type floating offshore wind turbines. A comprehensive multi-body dynamic model of the offshore wind turbine is developed for this purpose. Various wind-wave loading environments have been simulated to evaluate the performance of the passive TMDI under various conditions. A parametric study on two key parameters of the TMDI i.e., the mass ratio and the inerter ratio is conducted and presented in this paper to serve as design

guidelines for practical implementation.The results have indicated encouraging prospects for the use of TMDIs in the control of vibrations of wind turbine towers with implications for the wind energy industry.

2 | COUPLING OFFSHORE WIND TURBINE WITH TMDI

A multi-body dynamic model of an offshore wind turbine coupled with a TMDI is developed using Kane's method[28]. Kane's method, reduces the labour required to derive the equations of motion of a dynamic system. The equations of motion derived by Kane's method are simpler and more readily solveable by a computer, in comparison with earlier classical approaches. State of the art wind turbine simulation tools such as FAST[29] employs Kane's method to model offshore wind turbines. Kane's method presents a powerful vector approach that offers considerable advantages over the tradition Euler-Lagrangian formulation. The dynamic equations of motion of complicated systems can be obtained from kinematics. Therefore, a description of the kinematics of the system instead of the total energy is enough to enable derivation of the governing equations of motion.

For accurate modelling of a multi-body system like a offshore wind turbine, it is necessary that every component is defined in its local coordinate system and then referred back to the global, in this case, inertial reference frame denoted by $\hat{\boldsymbol{z}}$. Refer Figure 1 for the different reference frames. Hence, local coordinate systems are assigned to the platform ($\hat{\boldsymbol{a}}$), tower nodes, tower-top ($\hat{\boldsymbol{b}}$), nacelle ($\hat{\boldsymbol{d}}$), low-speed shaft ($\hat{\boldsymbol{c}}$), azimuth ($\hat{\boldsymbol{e}}$) and the blades ($\hat{\boldsymbol{g}}$). The blades have more than one coordinate system assigned to them. For detailed modelling of the blades, they are referred to their coned coordinate system ($\hat{\boldsymbol{i}}$) followed by the pitched coordinate system (not in picture). Aerodynamic loads are applied on the blade nodes that are not only coned and pitched but also rotated due to elastic deformation of the blades in out-of-plane and in-plane directions. The coordinate systems used (except the tower and blade element fixed coordinate systems and blade pitched coordinate system) are shown in Figure 1. The platform rotation and rotation of the elastic members (tower and blades) occurs simultaneously about more than one axis. This restricts the use of a simple Euler rotation matrix to establish transformation relations between two coordinate systems. Although advanced methods can be used to derive these transformation relations, the small magnitude of these angles allows the use of small angle approximation that makes a Euler 1-2-3 rotation matrix independent of the sequence of rotation. The resulting transformation matrix is not orthogonal, hence, singular value decomposition is used to obtain the nearest orthogonal transformation. The reader may refer[?] for details on this transformation.

By a direct result of Newton's law of motion, Kane's equations of motion for a simple holonomic multi-body system can be stated as[28]

$$F_k + F_k^* = 0 \qquad \text{for } k = 1, 2, \ldots N \tag{1}$$

where, N is the total number of degrees of freedom required to describe the complete kinematics of the wind turbine system. With a set of M rigid bodies characterized by reference frame N_i and center of mass point X_i, the *generalized active force* associated with the k^{th} degree of freedom is given as[28]

$$F_k = \sum_{i=1}^{M} \left[{}^E\mathbf{v}_k^{X_i} \cdot \mathbf{F}^{X_i} + {}^E\boldsymbol{\omega}_k^{N_i} \cdot \mathbf{M}^{N_i} \right] \tag{2}$$

where $\mathbf{F}^{X_i}$ is force vector acting on the center of mass of point X_i and $\mathbf{M}^{N_i}$ is the moment vector acting on the N_i rigid body. ${}^E\mathbf{v}_k^{X_i}$ and ${}^E\boldsymbol{\omega}_k^{N_i}$ are the partial linear and partial angular velocity of the point X_i and rigid body N_i respectively associated with the k^{th} degree of freedom in the inertial (E) reference frame. The *generalized inertia force* for k^{th} degree of freedom is given as

$$F_k^* = -\sum_{i=1}^{M} \left[{}^E\mathbf{v}_k^{X_i} \cdot \left(m^{N_i} {}^E\mathbf{a}^{X_i} \right) + {}^E\boldsymbol{\omega}_k^{N_i} \cdot {}^E\dot{\mathbf{H}}^{N_i} \right] \tag{3}$$

where it is assumed that for each rigid body N_i, the inertia forces are applied at the centre of the mass point X_i. ${}^E\dot{\mathbf{H}}^{N_i}$ is the time derivative of the angular momentum of rigid body N_i about its center of mass X_i in the inertial frame[28]. For the wind turbine model, the mass of the platform, tower, yaw bearing, nacelle, hub, blades, generator contributes to the total generalized inertia forces. Generalized active forces are the forces applied directly to the wind turbine system, forces that ensure constraint relationships between the various rigid bodies and internal forces within flexible members. Forces applied directly on the offshore wind turbine system include aerodynamic forces on the blades and the tower, hydrodynamic forces on the platform, mooring forces on the platform, gravitational forces, generator torque, high-speed shaft brake. Here it must be noted that gearbox friction forces are neglected. Yaw springs and damper contribute to forces that enforce constraint relationship between rigid bodies. Internal forces within flexible members include elasticity and damping in tower, blades and drive-train.

As can be observed from the above equations, the kinematic description, i.e., the position, velocity and acceleration vectors of all important points on the offshore wind turbine system is the key requirement. As shown in Figure 3a, the TMDI is placed at the tower-top denoted by the point O, and hence the position vector of the damper from the tower-top can be given as

$$r^{OD} = \begin{cases} q_D \hat{\mathbf{b}}_3 & \text{coupled to side-to-side direction} \\ q_D \hat{\mathbf{b}}_1 & \text{coupled to fore-aft direction} \end{cases} \tag{4}$$

where D denotes the center of mass of the damper and q_D is the displacement of the damper from its neutral position. The kinematics of the coupled system is derived which, although straightforward, can be extensive due to the complexity of the overall system. The mass of the damper contributes to the generalized inertia forces and the spring, damper and inerter contributes to the generalized active forces of the entire system. To describe the complete motion of the coupled offshore wind turbine TMDI system the degrees of freedom/generalized coordinates used are given in equation 5.

$$\begin{aligned} \mathbf{q} = \{ & q_{Sg} \;\; q_{Sw} \;\; q_{Hv} \;\; q_R \;\; q_P \;\; q_Y \;\; q_{TFA1} \;\; q_{TSS1} \;\; q_{TFA2} \;\; q_{TSS2} \;\; q_{yaw} \;\; q_{GeAz} \;\; q_{DrTr} \\ & q_{B1F1} \;\; q_{B1E1} \;\; q_{B1F2} \;\; q_{B2F1} \;\; q_{B2E1} \;\; q_{B2F2} \;\; q_{B3F1} \;\; q_{B3E1} \;\; q_{B3F2} \;\; q_D \} \end{aligned} \tag{5}$$

The subscripts define the degrees of freedom under consideration and are described in Appendix A. Once the linear and angular

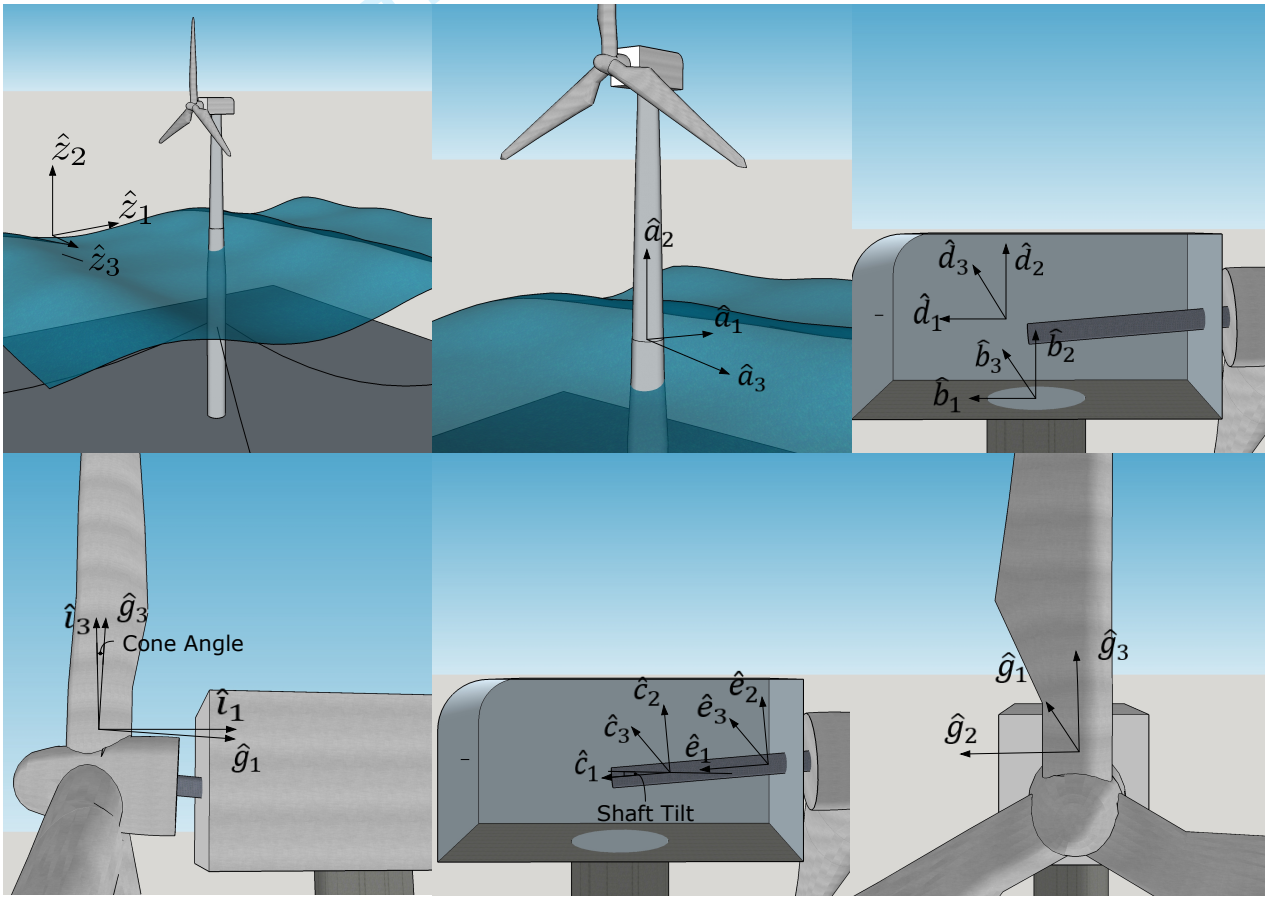

FIGURE 1 Coordinate systems

velocity vectors for every important point and rigid body in the system are defined, the partial linear and angular velocities are obtained as per[28] assuming the time derivatives of the generalized coordinates as the generalized speed (i.e., $u_k = \dot{q}_k$). The complete non-linear time-domain equations of motion for the offshore wind turbine system in its general form can be written as

$$\mathbf{M}(\mathbf{q}, \mathbf{u}, t)\dot{\mathbf{q}} = -\mathbf{f}(\dot{\mathbf{q}}, \mathbf{q}, \mathbf{u}, t) \tag{6}$$

where, **M** is the inertial mass matrix that is a non-linear function of the set of degrees of freedom **q**, control input **u**, and time t. The forcing function **f** depends non-linearly on the degrees of freedom, the time derivative of the degrees of freedom, control input and time.

2.1 | Dynamic loads

Aerodynamic loads

Aerodynamic loads on the wind turbine are estimated using steady Blade Element Momentum (BEM) theory. Three-dimensional (3D) wind fields are generated using the TurbSim[30] package distributed by National Renewable Energy Laboratory (NREL), USA. The wind fields generated by TurbSim account for vertical and horizontal wind shear and spatial coherence of the turbulent wind field. The package can be used to generate complete wind fields with varying turbulence intensity levels, power-law coefficients for wind shear and characteristic wind speeds. The steady BEM theory interpolates the wind speed at the blade nodes from the TurbSim generated 3D wind field to estimate aerodynamic loads based on the quasi-static aerodynamic properties (i.e., lift and drag) of the blades. This theory is widely available in the literature[31,32,33] and hence, it is not described in this paper. The BEM equations are solved using an approach proposed by Ning[34]. This approach solves for the unknown inflow angle instead of solving for the axial and the tangential induction factors as in earlier work. For this purpose, different equations are used in different solution regions (e.g. momentum, empirical or propeller brake region). Furthermore, the empirical region is estimated using Glauert's correction with Buhl's modification. Adjusting different equations for each region circumvents the traditional two-point iterative procedure of solving the BEM equations as described in[34]. Prandtl's hub and tip loss correction factors are also included to account for the vortices generated by the blade tips and the hub. The model is also capable of accounting for skewed inflow using a correction on the axial induction factor proposed by Pitt and Peters as obtained from[35]. The solution of the BEM equations at each section gives the elemental lift and drag forces. The elemental out-of-plane force (thrust) and in-plane force (torque) on the blade sections can be estimated from the elemental lift and drag forces. For details on the procedure please refer[35].

Hydrodynamic loads

Morison's representation is used to estimate hydrodynamic loads on the cylindrical spar of the floating wind turbine. In conjunction with strip theory, Morison's equations can be used to compute linear wave inertia forces and non-linear viscous drag forces. The total load on the platform is then obtained by integrating the elemental forces along the depth of the platform. The forces associated with a strip $\mathrm{d}z$ of the platform in surge and sway direction are given as

$$\mathrm{d}F_i^P(z,t) = \underbrace{-C_A\rho\left(\frac{\pi D(z)^2}{4}\right)\ddot{q}_i(z,t)\mathrm{d}z}_{\text{added mass}} + \underbrace{C_M\rho\left(\frac{\pi D(z)^2}{4}\right)a_i^f(z,t)\mathrm{d}z}_{\text{fluid inertial force}} + \underbrace{\frac{1}{2}C_D\rho D(z)\left(v_i^f(z,t)-v_i^p(z,t)\right)|v_i^f(z,t)-v_i^p(z,t)|\mathrm{d}z}_{\text{viscous drag force}} \quad \text{for } i = Sg, Sw \tag{7}$$

Where, the superscript 'P' denotes the platform and $\mathrm{d}F_i^P$ is the elemental force on the platform for the i^{th} degree of freedom. Similarly, the roll and pitch moments on the platform can be given as

$$\mathrm{d}M_i^P(z,t) = \begin{cases} -\mathrm{d}F_{Sg}^P(z,t)z & i = P \\ \mathrm{d}F_{Sw}^P(z,t)z & i = R \end{cases} \tag{8}$$

Where, $\mathrm{d}M_i^P$ is the elemental moment on the platform for the i^{th} degree of freedom. The total forces and moments on the platform are obtained by integration of the elmental forces and moments along the depth of the platfrom. Since, the spar is symmetrical about its vertical axis, the yaw moment and heave force are assumed to be zero. Morison's representation assumes that viscous drag force dominates the total drag force and radiation damping is negligible. This is valid only for rigid platforms with small motion, which is true in this case. Equation 7 does not include the added mass associated with the heave motion of the platform. Hence, added mass coefficient for heave degree of freedom is included as per[36].

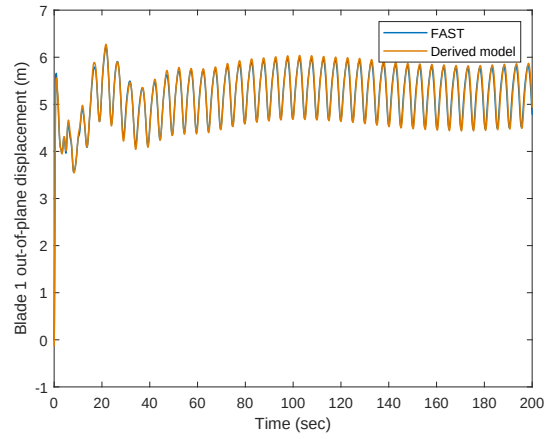

(a) Blade 1 out-of-plane displacement

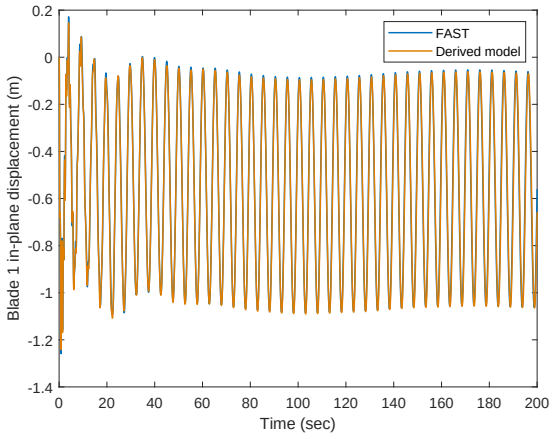

(b) Blade 1 in-plane displacement

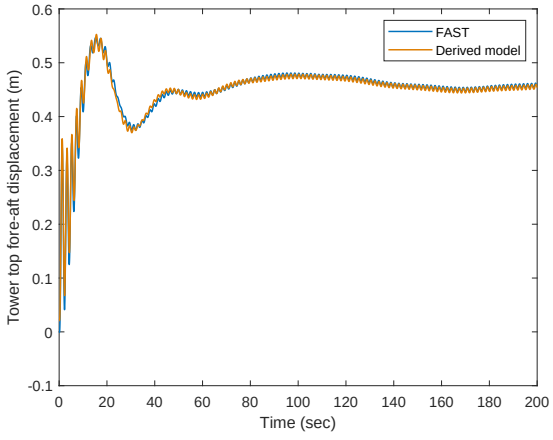

(c) Tower top fore-aft displacement

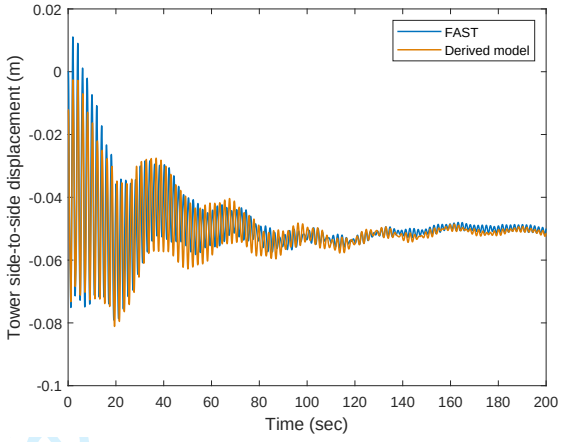

(d) Tower top side-to-side displacement

FIGURE 2 Model verification: motion of the wind turbine tower and blades

3 | MODEL VERIFICATION

The codes for the offshore wind turbine are developed in MATLAB ® [37]. The offshore wind turbine model developed is benchmarked against the state-of-the-art wind turbine simulator FAST [29]. FAST has been used in many previous studies on wind turbine dynamics and control [38 39 8] and is verified and validated by DNV GL [40]. The spar-type offshore wind turbine defined in [41] is used for analysis. The verification results are shown in Figure 2 and in Appendix B. For brevity only the main structural responses are shown in Figure 2. The other responses of the offshore wind turbine are provided in Appendix B. The offshore wind turbine is simulated under steady rated wind speed of 11.4 m/s in still water.

An excellent similarity is observed for the wind turbine tower, nacelle and blade motion while some dissimilarities are observed in the platform motion. The main difference is a phase shift in the response time histories. This is due to the fact that while FAST applies hydrodynamic damping from both linear potential flow theory and viscous drag forces from Morison's equation, the derived model in this paper uses only viscous drag forces from Morison's equation. This difference in hydrodynamic damping results in a phase shift in the response time histories. Also, the degrees of freedom that experience less hydrodynamic damping like platform surge, heave or reaches steady state quickly like platform pitch, yaw is less affected by the phase shift. The platform sway and roll degrees of freedom experience a noticeable phase shift due to the difference in hydrodynamic damping. However, the mean and the frequency content of the responses remain the same which is important from a dynamic analysis point of view.

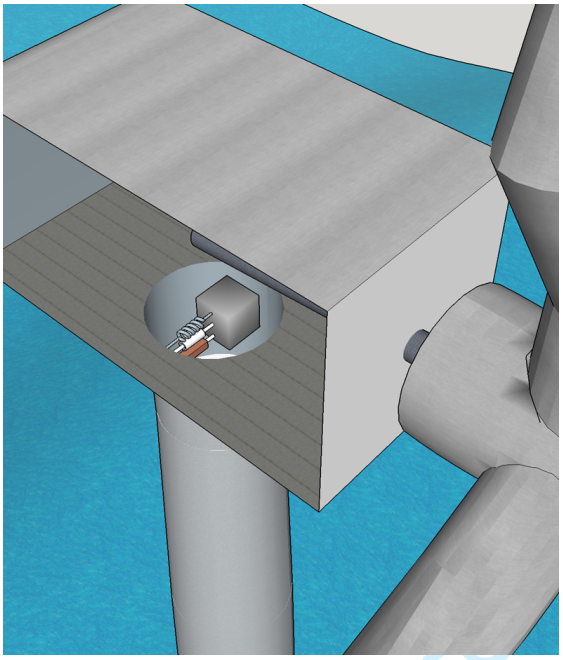

(a) Offshore wind turbine tower coupled with TMDI

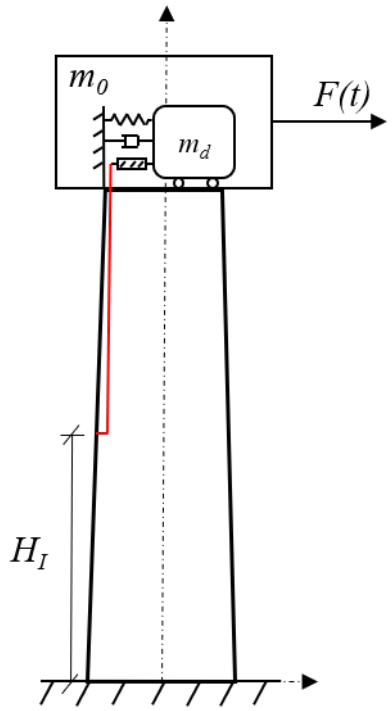

(b) Schematic diagram of a tower with a TMDI placed on the top

FIGURE 3

4 | DAMPER OPTIMIZATION USING A REDUCED MODEL

The coupled offshore wind turbine TMDI system presents a rather complicated set of equations of motion for which optimization of damper properties in closed form is not possible. Therefore, the optimal properties of the TMDI are derived using a simple reduced model subjected to white noise excitation. The simplified model of a tower with a TMDI placed on its top is shown in Figure 3b. It is assumed that the mass of the blades, hub and nacelle are lumped on the top of the tower and the base of the tower is fixed. The inerter is hooked between the mass of the damper and the tower at an arbitrary height H_I from the base of the tower. It is also assumed that the primary structure does not offer any damping force. For such a system, the governing equations of motion normalized by the mass of the primary structure m_0 is given as

$$\begin{bmatrix} 1+\mu+\beta(1-\phi)^2 & \mu+\beta(1-\phi) \\ \mu+\beta(1-\phi) & \mu+\beta \end{bmatrix} \begin{pmatrix} \ddot{q}_t \\ \ddot{q}_d \end{pmatrix} + \begin{bmatrix} 0 & 0 \\ 0 & 2\mu\omega_t\zeta_d\omega_r \end{bmatrix} \begin{pmatrix} \dot{q}_t \\ \dot{q}_d \end{pmatrix} + \begin{bmatrix} \omega_t^2 & 0 \\ 0 & \mu\omega_t^2\omega_r^2 \end{bmatrix} \begin{pmatrix} q_t \\ q_d \end{pmatrix} = \begin{pmatrix} \frac{F}{m_0} \\ 0 \end{pmatrix} \tag{9}$$

The tower and damper degrees of freedom are denoted by q_t and q_d respectively. The mass ratio of μ and inerter ratio β are defined as

$$\mu = \frac{m_d}{m_0} \qquad \beta = \frac{b}{m_0} \tag{10}$$

where m_d is the mass of the damper and b is the constant of proportionality of the force generated by the inerter. It has the units of mass and details on this parameter can be found in[22,42]. The natural frequency of the tower and damper is denoted by ω_t and ω_d respectively. The tuning ratio and damping ratio of the damper are defined as

$$\omega_r = \frac{\omega_d}{\omega_t} \qquad \zeta_d = \frac{c_d}{2m_d\omega_d} \tag{11}$$

where c_d is the damping coefficient of the TMDI. ϕ is the normalized displacement ratio between tower top displacement and the displacement at a height H_I from the base. It can be obtained directly from the normalized primary mode shape as

$$\phi = \phi_t(H_I) \qquad \text{where } 0 \le \phi \le 1 \tag{12}$$

where, ϕ_t is the normalized primary mode shape of the tower. F is the stationary stochastic excitation force. The excitation force is assumed to be white with a constant intensity of S_0 over all frequencies. For this case the variance of the tower can be given as

$$\sigma_t^2 = \frac{1}{m_0}\int_{-\infty}^{+\infty} |\Lambda_{11}(\omega)|^2 S_0 \mathrm{d}\omega \tag{13}$$

where, Λ_{11} is the first component of the transfer function matrix that can be obtained from equation 9 as

$$\Lambda(i\omega) = [-\omega^2 M + i\omega C + K]^{-1} \tag{14}$$

Using an analytical technique as per[43] equation 13 can be obtained as

$$\sigma_t^2 = \frac{\pi S_0}{m_0}\frac{\begin{vmatrix} 0 & b_2 & b_1 & b_0 \\ -d_4 & d_2 & -d_0 & 0 \\ 0 & -d_3 & d_1 & 0 \\ 0 & d_4 & -d_2 & d_0 \end{vmatrix}}{\begin{vmatrix} d_3 & -d_1 & 0 & 0 \\ -d_4 & d_2 & -d_0 & 0 \\ 0 & -d_3 & d_1 & 0 \\ 0 & d_4 & -d_2 & d_0 \end{vmatrix}} \tag{15}$$

where

$$\begin{aligned}
b_0 &= \mu^2\omega_t^4\omega_r^4 \\
b_1 &= 2\mu\omega_t^2\omega_r^2(2\mu\zeta_d^2 - \mu - \beta) \\
b_2 &= \mu^2 + 2\mu\beta + \beta^2 \\
d_0 &= \mu\omega_t^4\omega_r^2 \\
d_1 &= 2\mu\omega_t^3\zeta_d\omega_r \\
d_2 &= -\omega_t^2(-\mu^2\omega_r^2 - \mu\phi^2\beta\omega_r^2 + 2\mu\phi\beta\omega_r^2 - \mu\beta\omega_r^2 - \mu\omega_r^2 - \mu - \beta) \\
d_3 &= -2\mu\omega_t\zeta_d\omega_r(-\mu - \phi^2\beta + 2\phi\beta - \beta - 1) \\
d_4 &= -2\mu\omega_t\zeta_d\omega_r(-\mu - \phi^2\beta + 2\phi\beta - \beta - 1)
\end{aligned}$$

The optimal TMDI parameters can be then obtained as

$$\frac{\partial\sigma_t^2}{\partial\omega_r} = 0 \qquad \frac{\partial\sigma_t^2}{\partial\zeta_d} = 0 \tag{16}$$

Assuming that the mass ratio μ, inerter ratio β and ϕ are held constant the equations in 16 lead to the optimal tuning ratio

$$\omega_r = \sqrt{\frac{-B + \sqrt{B^2 - A * C}}{2A}} \tag{17}$$

where

$$\begin{aligned}
A &= 3\mu^2(\mu^2 + 2\mu\phi^2\beta - 4\mu\phi\beta + 2\mu\beta + 2\mu + \phi^4\beta^2 - 4\phi^3\beta^2 + 6\phi^2\beta^2 + 2\phi^2\beta - 4\phi\beta^2 - 4\phi\beta + \beta^2 + 2\beta + 1) \\
B &= \mu(4\mu^2\zeta_d^2 - \mu^2 + 4\mu\phi^2\zeta_d^2\beta - 2\mu\phi^2\beta - 8\mu\phi\zeta_d^2\beta + 2\mu\phi\beta + 4\mu\zeta_d^2\beta + 4\mu\zeta_d^2 - 2\mu\beta - 2\mu - \phi^2\beta^2 + 2\phi\beta^2 \\
&\quad - \beta^2 - 2\beta) \\
C &= -(\mu^2 + 2\mu\beta + \beta^2)
\end{aligned}$$

and the optimal damping ratio

$$\zeta_d = \frac{1}{2\mu\omega_r}\sqrt{\frac{D}{E}} \tag{18}$$

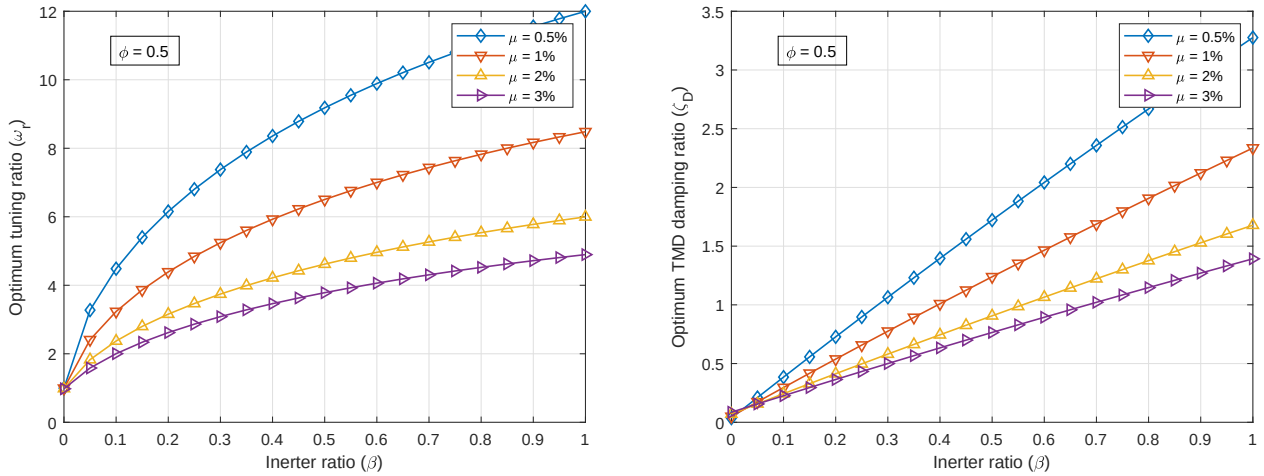

(a) Optimum tuning ratio **(b)** Optimum damping ratio

FIGURE 4 Optimum TMDI parameter for $\phi = 0.5$.

where

$$D = \mu^4\omega^4 + 2\mu^3\phi^2\beta\omega_r^4 - 4\mu^3\phi\beta\omega_r^4 + 2\mu^3\beta\omega_r^4 + 2\mu^3\omega_r^4 - \mu^3\omega_r^2 + \mu^2\phi^4\beta^2\omega_r^4 - 4\mu^2\phi^3\beta^2\omega_r^4 + 6\mu^2\phi^2\beta^2\omega_r^4 + 2\mu^2\phi^2\beta\omega_r^4 - 2\mu^2\phi^2\beta\omega_r^2 - 4\mu^2\phi\beta^2\omega_r^4 - 4\mu^2\phi\beta\omega_r^4 + 2\mu^2\phi\beta\omega_r^2 + \mu^2\beta^2\omega_r^4 + 2\mu^2\beta\omega_r^4 - 2\mu^2\beta\omega_r^2 + \mu^2\omega_r^4 - 2\mu^2\omega_r^2 + \mu^2 - \mu\phi^2\beta^2\omega_r^2 + 2\mu\phi\beta^2\omega_r^2 - \mu\beta^2\omega_r^2 - 2\mu\beta\omega_r^2 + 2\mu\beta + \beta^2$$

$$E = \mu + \phi^2\beta - 2\phi\beta + \beta + 1$$

It is important to note that when $b = \beta = 0$ the equations 17 and 18 reduce to the optimal tuning parameters for a classical TMD coupled to a primary structure excited by white noise. Since ϕ is an independent parameter, the optimal parameters for the TMDI can be obtained directly from the above equations when the inerter is hooked at an arbitrary height. It is also important to note that equations 17 and 18 are interdependent. Hence, the optimum parameters cannot be obtained in one step and an iterative procedure must be used until the two parameters converge with a sufficiently small tolerance.

In the following optimal tuning ratio ω_r and optimal damping ratio ζ_d at different values of mass, inerter and tip displacement ratios are shown in Figure 4 and Figure 5. It can be observed that the tuning parameters are significantly different from those of a classical TMD. Very high tuning ratios and damping ratios are required for optimum performance when β is increased from 0 to 1. At $\beta = 0$ the optimum parameters match that of a classical TMD, as expected. Figures6 through 9 show the minimum variance ratio between a TMDI with $b = 0$ (classical TMD) and $b > 0$ for different β and ϕ. The important points to note from these plots are - (i) the performance improves with increased β and decreased ϕ, therefore, the lower the inerter hook on the tower and higher the inerter ratio the better; (ii) for $\phi > 0.8$, in most cases, the performance is worse compared to a classical TMD, therefore, the inerter is essentially ineffective; and; (iii) the minimum variance ratio saturates with increasing β and decreasing ϕ, therefore, it is the designer's decision to choose an optimum value for these two parameters based on desired performance and practical/physical restrictions of the structure.

5 | CONTROLLER PERFORMANCE

To evaluate the performance of the passive TMDI the damper is coupled to the derived model represented by Eq. 6 using Kane's method. The coupling is preformed in the side-to-side and fore-aft directions one at a time and the results are presented in this section. A few representative met-ocean conditions are selected to represent calm and violent conditions. To represent calm conditions small waves of $H_s = 0.75$ m are selected with a wave period of $T_p = 6$ sec. It is assumed that small wave heights are accompanied by low wind speeds. Similarly, to represent violent environmental conditions large waves of $H_s = 6$ m along with high wind speeds are assumed. Every wind-wave condition is simulated with a wave direction of 0 and 90 degrees.

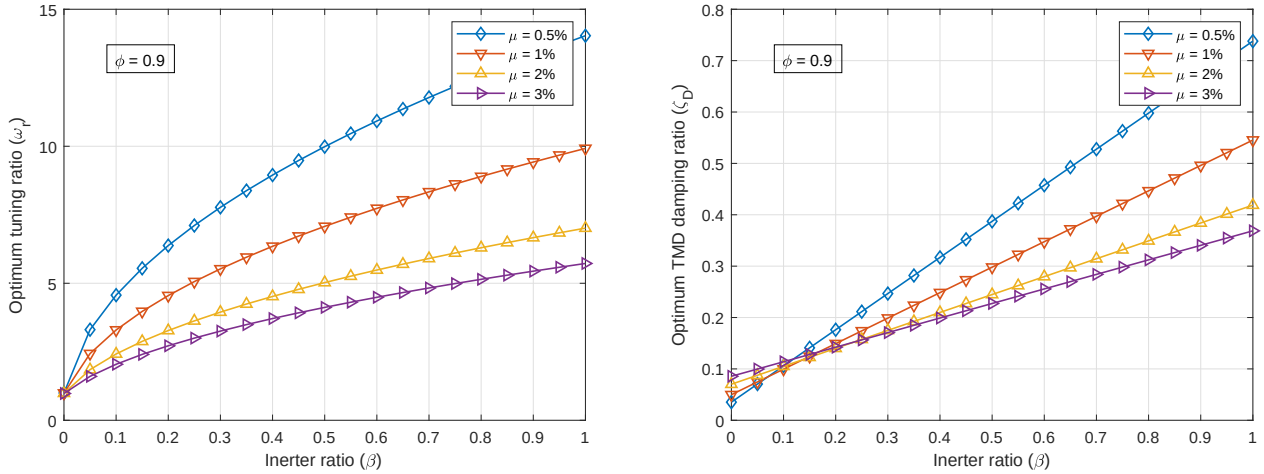

(a) Optimum tuning ratio **(b)** Optimum damping ratio

FIGURE 5 Optimum TMDI parameter for $\phi = 0.9$.

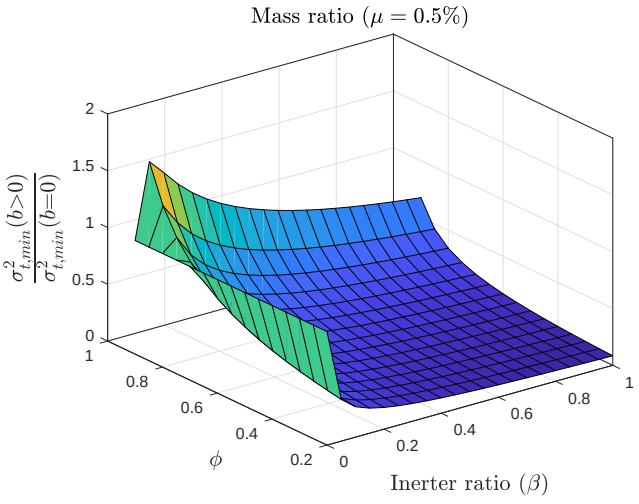

FIGURE 6 Minimum variance ratio between TMDI with $\beta = 0$ and $\beta > 0$ for $\mu = 0.5\%$.

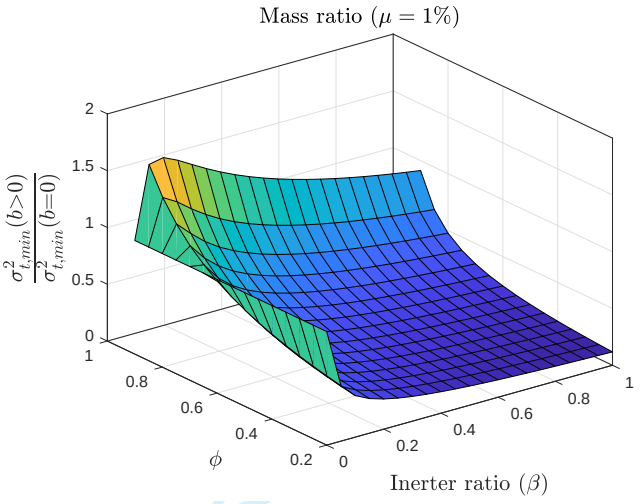

FIGURE 7 Minimum variance ratio between TMDI with $\beta = 0$ and $\beta > 0$ for $\mu = 1\%$.

Resonance of the tower response is another aspect that needs to be investigated. Since the tower frequency is ≈ 0.4885 Hz the wave period needs to be ≈ 2.05 sec. It is known from literature[44,45] that waves of such short periods are highly improbable and hence resonance with wave excitation frequency is ignored. However, aerodynamic loads can resonate with the tower's natural frequency when 3P ≈ 0.4885 Hz $\Rightarrow$ P ≈ 0.163 Hz; i.e., at a rotor speed of ≈ 9.78 rpm. Since 9.78 rmp falls within the operational range of the wind turbine this case is also investigated although the wind speed varies constantly and a constant rmp of 9.78 cannot be maintained. Table 1 and Table 2 shows the performance of the passive TMDI for the aforementioned wind-wave environmental conditions in controlling the side-to-side and fore-aft displacements of the tower. The mass ratio of the TMDI is fixed at 1% and the inerter is hooked to the tower at a height of 54 m from the base of the tower that gives $\phi = 0.5$. It can be clearly observed that considerable gain in performance is obtained when an inerter is attached to the tuned mass damper. As expected the performance improves with an increase in the inerter ratio β and the behaviour is the same for all the investigated loading environments. It is also noticeable that the performance of the TMDI does not improve or rather marginally deteriorates in some cases when the inerter ratio is increased from 0.4 to 0.8. It is known from recent literature[22] and from the previous

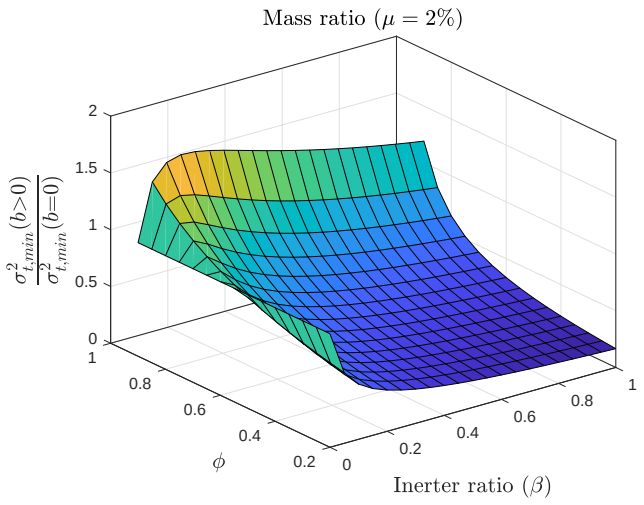

FIGURE 8 Minimum variance ratio between TMDI with $\beta = 0$ and $\beta > 0$ for $\mu = 2\%$.

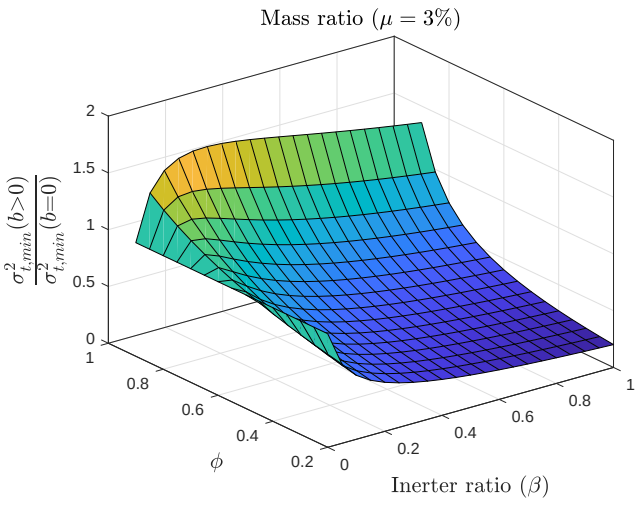

FIGURE 9 Minimum variance ratio between TMDI with $\beta = 0$ and $\beta > 0$ for $\mu = 3\%$.

Section that the performance of the TMDI saturates as β is increased. The performance saturates from $\beta = 0.4$ to $\beta = 0.8$. The exact behaviour of this saturation is studied in detail later. Another noticeable impact of installing an inerter is a large reduction in TMD stroke. Large TMD stroke is always a hindrance in the installation of these devices on actual structures. Researches, therefore, have utilised the concept of TMDs with stroke constraints. But, the simple installation of an inerter in parallel with the spring and damper of the TMD can drastically reduce (approximately by 90%) the stroke of the TMD and this can be a major asset in the practical installation of TMDs especially on structures such as wind turbines where space constraints are a concern.

Figure 10 through Figure 19 show the Fourier spectrum of the tower side-to-side and fore-aft displacement for the load cases and damper properties defined in Table 1 and Table 2. The drastic reduction of TMDI stroke is visualized in Figure 10b and Figure 11b. The qualitative behaviour of stroke reduction is similar for all other load cases and hence is not shown in this paper. The quantitative reduction in the peak value of TMDI stroke is provided in the tables. Important things to note from the Fourier spectra are listed below:

- The roll and pitch degrees of freedom of the platform affects the dynamics of the tower in the side-to-side and fore-aft directions respectively.
- Wave directions of 90 degrees and 0 degrees have a considerable effect on the dynamics of the tower side-to-side and fore-aft motion respectively even though the wave excitation frequency does not resonate with the natural frequency of the tower. And of course, larger waves have a bigger effect.
- Energy associated with the tower side-to-side natural frequency is considerably higher compared to the tower fore-aft natural frequency and hence the reductions obtained in the side-to-side direction are greater. The tower in the fore-aft direction experiences a larger amount of aerodynamic damping, explaining this behaviour.
- The optimum tuning parameters obtained in the previous section, although approximate, provide very good tuning as the damper is capable of almost entirely damping out the energy associated with the tower's natural frequency.

5.1 | Parametric study: On TMDI mass ratio and inerter ratio

The results provided above establishes the fact that the passive TMDI system performs well in different loading environments. Now it is of interest to investigate the sensitivity of the two key parameters (i.e., the mass ratio μ and inerter ratio β). The primary aim of this investigation is to identify the parameters at which a heavier classical TMD can be replaced by a lighter TMDI while maintaining, or even improving upon, the performance of the damper. A nominal wind-wave loading environment is chosen for this investigation. Rated hub height wind speed of 11.4 m/s along with wave height and a wave period of 2.25 m and 6.25 sec are

TABLE 1 Tower side-to-side response and controller performance.

LC	Description	U_w	H_s	T_p	Wave dir.	W/O TMDI	W/ TMDI								
							$\beta = 0$			$\beta = 0.4$			$\beta = 0.8$		
						q_T^{RMS}	q_T^{RMS}	q_D^{max}	$P.R$	q_T^{RMS}	q_D^{max}	$P.R$	$S.R$	q_T^{RMS}	q_D^{max}	$P.R$	$S.R$
1.1	Violent met-ocean condition; high wind speeds with large wave heights	20	6	8	0	0.050	0.031	0.409	38%	0.024	0.043	53%	90%	0.023	0.026	55%	94%
1.2					90	0.176	0.143	1.191	19%	0.135	0.191	23%	84%	0.139	0.149	21%	88%
2.1	Calm met-ocean condition; low wind speeds with small wave heights	8	0.75	6	0	0.014	0.010	0.115	32%	0.007	0.009	51%	92%	0.007	0.006	53%	95%
2.2					90	0.034	0.024	0.286	29%	0.020	0.041	41%	86%	0.021	0.036	39%	87%
3	Resonance of tower with aerodynamic loads	8.8	2.25	6.25	90	0.094	0.065	0.746	31%	0.056	0.089	40%	88%	0.058	0.096	38%	87%

*$S.R$ = Percentage reduction in TMD stroke

*$P.R = \left(1 - \frac{q_T^{con}}{q_T^{uncon}}\right) 100\%$

*$\phi = 0.5$

TABLE 2 Tower fore-aft response and controller performance.

LC	Description	U_w	H_s	T_p	Wave dir.	W/O TMDI	W/ TMDI							
							$\beta = 0$			$\beta = 0.4$			$\beta = 0.8$		
						q_T^{RMS}	q_T^{RMS}	q_D^{max}	$P.R$	q_T^{RMS}	q_D^{max}	$P.R$	$S.R$	q_T^{RMS}	q_D^{max}	$P.R$	$S.R$
1.1	Violent met-ocean condition; high wind speeds with large wave heights	20	6	8	0	0.154	0.153	1.128	1%	0.150	0.164	2%	85%	0.154	0.139	0%	88%
1.2					90	0.077	0.075	0.743	3%	0.066	0.122	15%	84%	0.064	0.071	17%	90%
2.1	Calm met-ocean condition; low wind speeds with small wave heights	8	0.75	6	0	0.055	0.053	0.463	4%	0.046	0.067	16%	86%	0.046	0.048	17%	90%
2.2					90	0.052	0.050	0.479	5%	0.043	0.052	18%	89%	0.042	0.030	20%	94%
3	Resonance of tower with aerodynamic loads	8.8	2.25	6.25	0	0.081	0.079	0.592	3%	0.074	0.114	9%	81%	0.075	0.092	8%	84%

*$S.R$ = Percentage reduction in TMD stroke
*$P.R = \left(1 - \frac{q_T^{con}}{q_T^{uncon}}\right) 100\%$
*$\phi = 0.5$

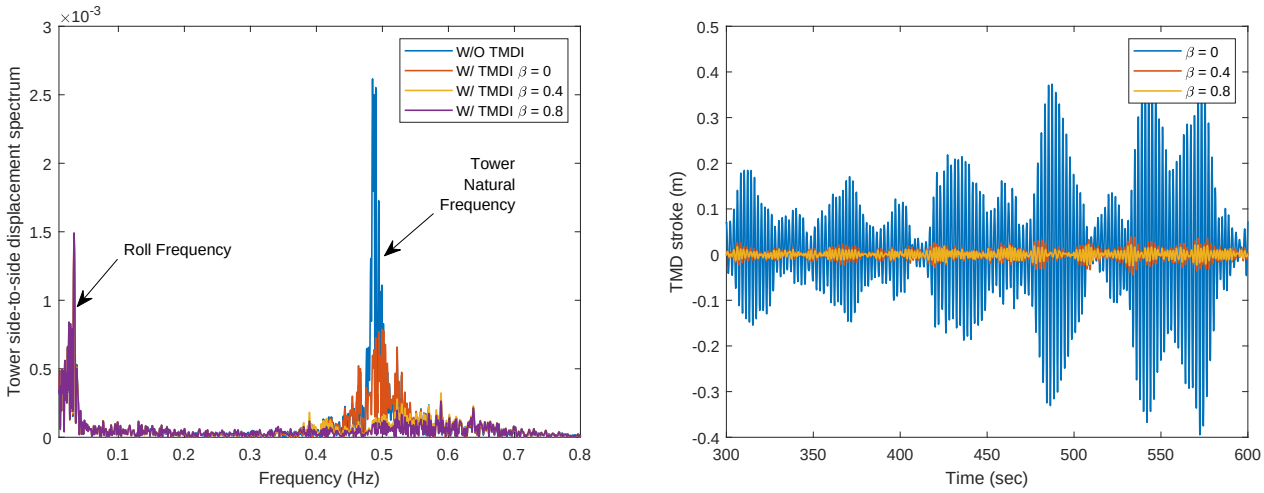

(a) Tower side-to-side response spectrum **(b)** TMD stroke (m) with and without inerter

FIGURE 10 Load Case 1.1: Uncontrolled and controlled tower side-to-side response and TMD stroke

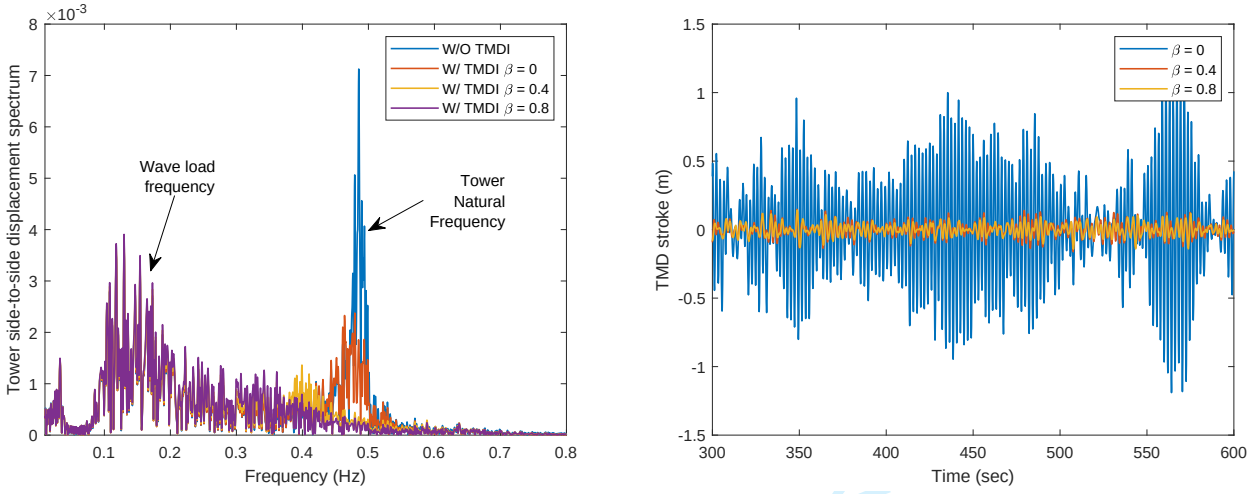

(a) Tower side-to-side response spectrum **(b)** TMD stroke (m) with and without inerter

FIGURE 11 Load Case 1.2: Uncontrolled and controlled tower side-to-side response and TMD stroke

selected. Simulations are performed for various mass ratios and inerter ratios and the reduction obtained in fore-aft and side-to-side response of the tower are presented in Figure 20 and Figure 21 respectively. It can be observed that the performance sharply increases initially when β is increased but also saturates very quickly when $\beta \gtrapprox 0.2$. This shows that increasing β indefinitely will not have any significant improvement in the performance.

However, the key thing to note from the curves is that although the performance increase for increased mass ratio when $\beta = 0$, the performance eventually drops when a $\beta > 0$ is introduced, and a TMDI with smaller mass ratio works better than a TMDI with a larger mass ratio. This behaviour is unlike fixed base structures as available in literature[22,42]. To investigate this behaviour, further investigation was carried on into the platform motion with increasing mass ratio of the damper. Understandably, the motion of the platform increases when a heavier mass is placed on top of the tower. A quantitative estimate of the increase in the roll and pitch of the platform is provided in Figure 22. It shows that with increasing mass ratio of the TMDI the roll and the pitch of the platform also increases linearly. This increase in platform vibrations is reflected in the increase of tower vibrations and hence the reduction in performance of the damper. Hence, for an offshore wind turbine tower it is not ideal to increase the mass

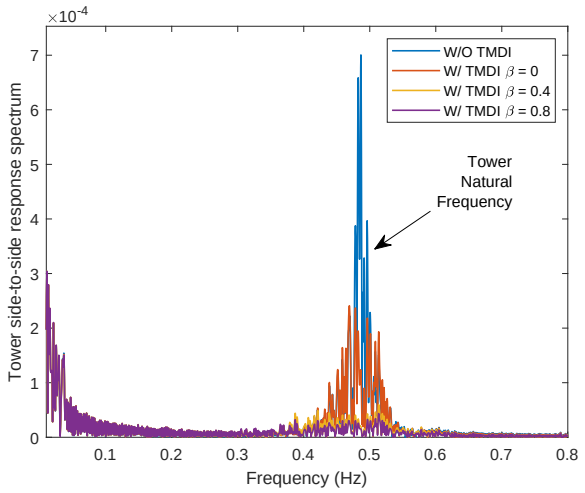

FIGURE 12 Load Case 2.1: Uncontrolled and controlled tower side-to-side response spectrum

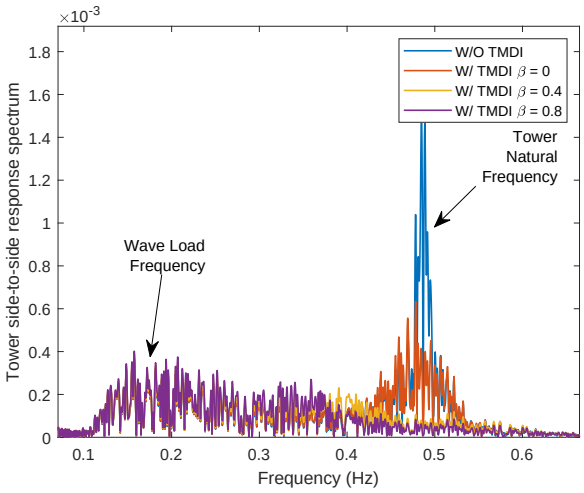

FIGURE 13 Load Case 2.2: Uncontrolled and controlled tower side-to-side response spectrum

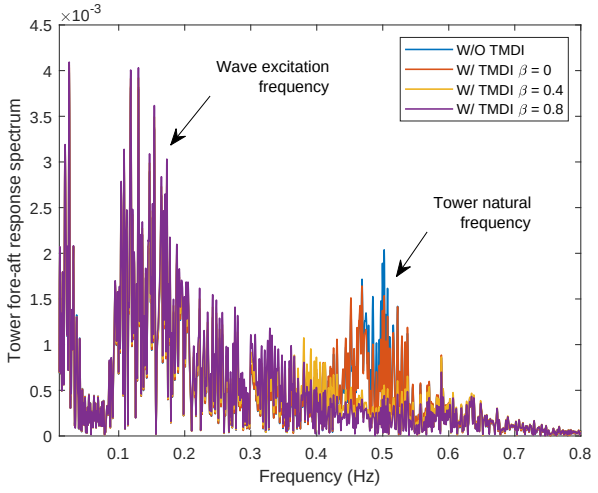

FIGURE 14 Load Case 1.1: Uncontrolled and controlled tower fore-aft response spectrum

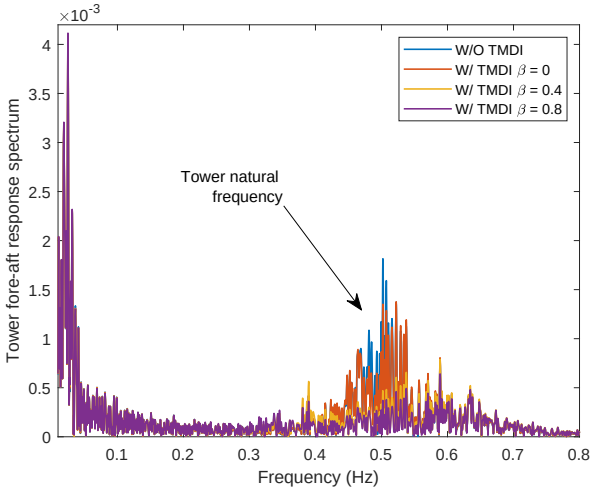

FIGURE 15 Load Case 1.2: Uncontrolled and controlled tower fore-aft response spectrum

ratio of a passive damper to improve performance not only because of spatial restrictions at the top of the tower but also because it will result in increased vibrations of the overall system. A TMDI with low mass ratio and a high inerter ratio is recommended.

It is well known from literature[46] that the blades and the tower are dynamically coupled. Therefore the effect of tower vibration reduction on the blades must be studied. For that purpose, the tower fore-aft displacement and the blade out-of-plane displacement is shown in Figure 23 and Figure 24 respectively subjected to load case 2.1. The dynamic coupling between the blades and the tower can be clearly observed as the change in tower motion is reflected in the blade response. However, even though the reduction in the tower fore-aft vibrations alters the blade out-of-plane tip displacement, the blade out-of-plane response is not mitigated by the presence of a damper at the tower top.

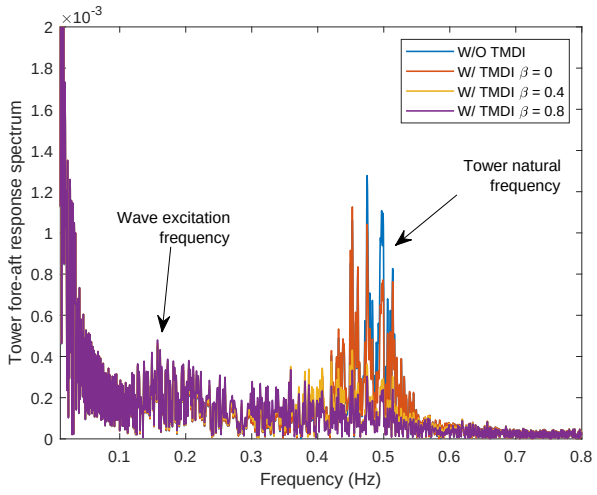

FIGURE 16 Load Case 2.1: Uncontrolled and controlled tower fore-aft response spectrum

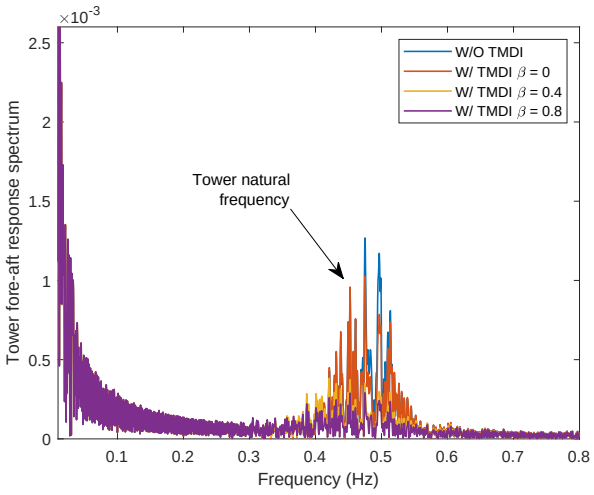

FIGURE 17 Load Case 2.2: Uncontrolled and controlled tower fore-aft response spectrum

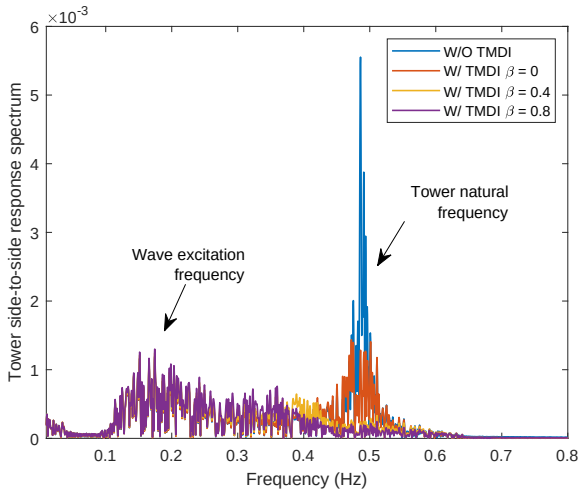

FIGURE 18 Load Case 3: Uncontrolled and controlled tower side-to-side response spectrum

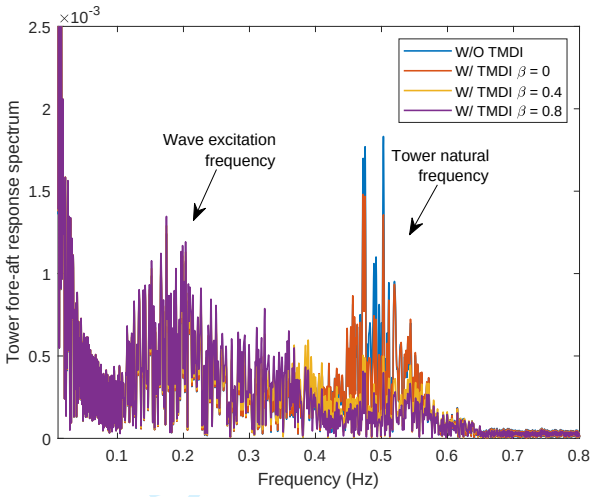

FIGURE 19 Load Case 3: Uncontrolled and controlled tower fore-aft response spectrum

6 | CONCLUSIONS

Passive vibration control of a spar-type floating offshore wind turbine tower using tuned mass-damper-inerter has been investigated in detail in this paper using a comprehensive multi-body dynamic model of the offshore wind turbine. Various wind-wave loading environments have been simulated to evaluate the performance of the controller under various conditions. A parametric study on the two key parameters of the TMDI i.e., the mass ratio and the inerter ratio, has been conducted and presented in this paper to serve as design guidelines for practical implementation. The key highlights can be summarized as follows

- For a fixed mass ratio (μ) the performance of the TMDI improves with an increasing inerter ratio (β), highlighting the fact that a heavier classical TMD can be easily replaced by a TMDI of smaller mass.
- Although the performance of a TMDI increases with increasing β, it has been found that the improvement saturates above a value of 0.4. Hence, an inerter ratio higher than 0.4 is generally not required and very good performance can be achieved with a low inerter ratio of 0.1 to 0.2.

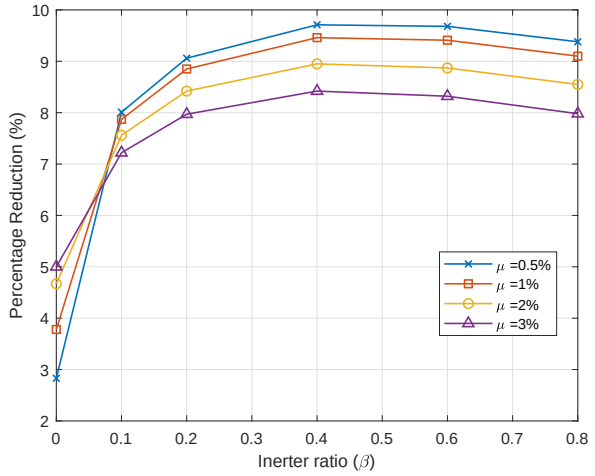

FIGURE 20 Percentage reduction at different mass and inerter ratios

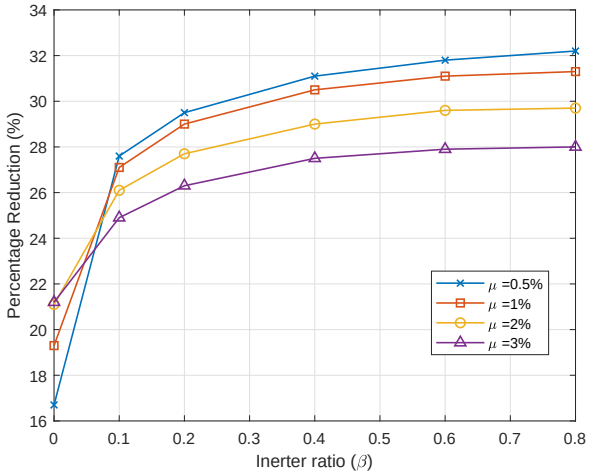

FIGURE 21 Percentage reduction at different mass and inerter ratios

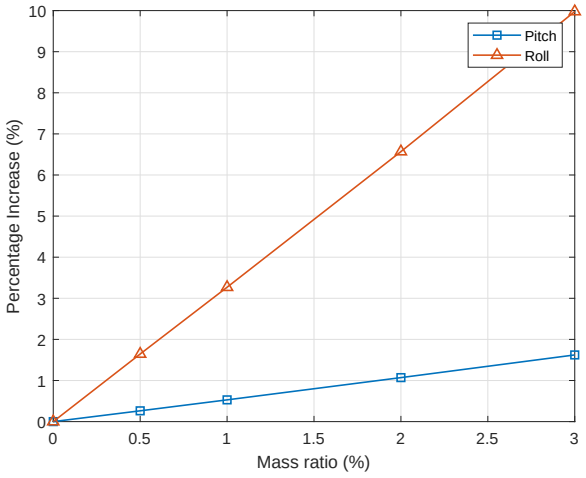

FIGURE 22 Percentage increase in standard deviation of platform pitch and roll at various mass ratios

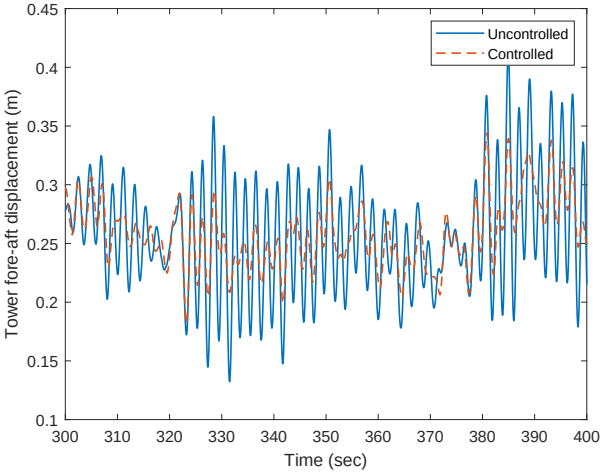

FIGURE 23 Load case 2.1: Tower fore-aft response

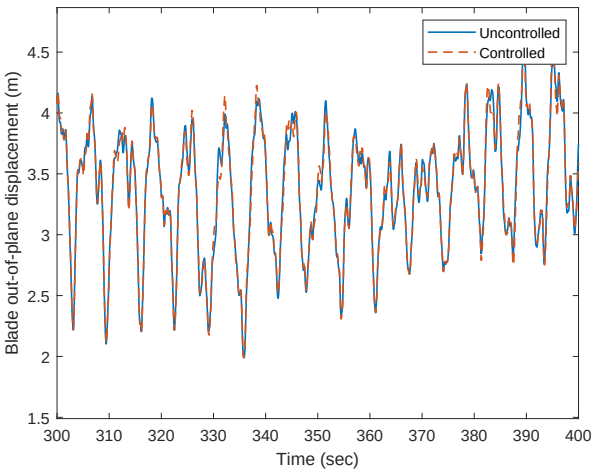

FIGURE 24 Load case 2.1: Blade out-of-plane response

- The optimum tuning parameters presented in this paper are derived for a simplified fixed base tower subjected to white noise excitation. It has been shown that these tuning parameters are capable of damping out the energy associated with the tower's natural frequency almost completely. Therefore, these parameters can be used for a floating offshore wind turbine tower with sufficient reliability.
- Impressive response reductions of about 10% and 32% in tower fore-aft and side-to-side directions respectively are achieved in the nominal case and reductions of up to 18% and 53% in the two respective directions have been observed in the most extreme cases.
- Unlike vibration control of a building or fixed base tower, the performance of the TMDI drops for higher mass ratio when $\beta > 0$. An investigation into this behaviour revealed that increasing the mass at the top of the tower increases the motion of the platform (increased platform pitch and roll) which in turn results in larger vibrations of the tower. Therefore, unlike traditional civil engineering structures, it is very important that for an offshore wind turbine tower a TMDI with a smaller mass ratio and a higher inerter ratio is used to achieve maximum performance.
- Another key benefit observed from the introduction of an inerter is the drastic reduction in TMD stroke. Large TMD stroke is a practical hindrance in the installation of classical TMDs in structures. A huge reduction in TMD stroke of about 90% has been observed consistently by the introduction of an inerter in the system. This along with improved vibration control properties (when tuned properly) offered by a tuned mass-damper-inerter makes it an exciting candidate for passive vibration control of offshore wind turbines with space constraints.

APPENDIX

A DEGREES OF FREEDOM

The complete nonlinear floating offshore wind turbine model has 22 degrees of freedom. Six degrees of freedom are used to describe the motion of the platform. Four degrees of freedom to describe the motion of the tower. One degree of freedom is used to describe the rotation of the nacelle. The rotation of the low speed shaft is modeled using two degrees of freedom. And nine degrees of freedom are used to describe the motion of the three blades. The degrees of freedom are listed in Table A1.

B MODEL VERIFICATION RESULTS

The derived model is benchmarked against FAST[29] and the motion of the nacelle, low-speed-shaft and the platform are is shown in Figure B1 and Figure B2.

References

1. Dueñas-Osorio L, Basu B. Unavailability of wind turbines due to wind-induced accelerations. *Engineering Structures* 2008; 30(4): 885–893.
2. Zhang Z, Basu B, Nielsen SR. Tuned liquid column dampers for mitigation of edgewise vibrations in rotating wind turbine blades. *Structural Control and Health Monitoring* 2015; 22(3): 500–517.
3. Zhang Z, Nielsen SR, Basu B, Li J. Nonlinear modeling of tuned liquid dampers (TLDs) in rotating wind turbine blades for damping edgewise vibrations. *Journal of Fluids and Structures* 2015; 59: 252–269.
4. Colwell S, Basu B. Tuned liquid column dampers in offshore wind turbines for structural control. *Engineering Structures* 2009; 31(2): 358 - 368. doi: 10.1016/j.engstruct.2008.09.001

TABLE A1 Degrees of freedom

q_{Sg}	Platform surge
q_{Sw}	Platform sway
q_{Hv}	Platform heave
q_R	Platform roll
q_P	Platform pitch
q_Y	Platform yaw
q_{TFA1}	First tower fore-aft bending mode
q_{TFA2}	Second tower fore-aft bending mode
q_{TSS1}	First tower side-to-side bending mode
q_{TSS2}	Second tower side-to-side bending mode
q_{yaw}	Nacelle yaw
q_{GeAz}	Generator azimuth angle
q_{DrTr}	Drive-train torsional flexibility
q_{BiF1}	First flapwise bending mode for i^{th} blade
q_{BiF2}	Second flapwise bending mode for i^{th} blade
q_{BiE1}	First edgewise bending mode for i^{th} blade
q_D	Damper

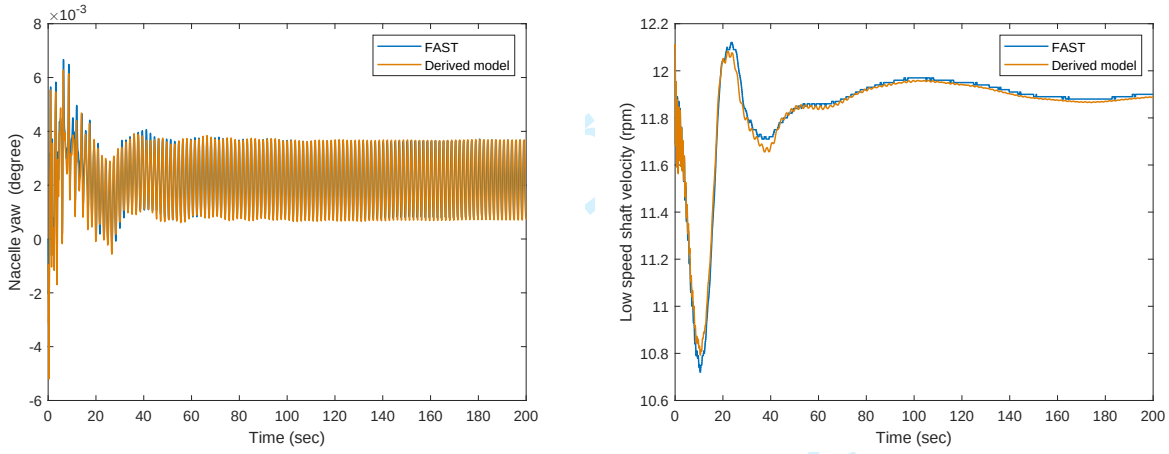

(a) Nacelle yaw rotation **(b)** Low speed shaft speed

FIGURE B1 Model verification: motion of the wind turbine nacelle and low-speed-shaft

5. Basu B, Zhang Z, Nielsen SR. Damping of edgewise vibration in wind turbine blades by means of circular liquid dampers. *Wind Energy* 2016; 19(2): 213–226.

6. Zhang Z, Li J, Nielsen SR, Basu B. Mitigation of edgewise vibrations in wind turbine blades by means of roller dampers. *Journal of Sound and Vibration* 2014; 333(21): 5283–5298.

7. Murtagh PJ, Ghosh A, Basu B, Broderick BM. Passive control of wind turbine vibrations including blade/tower interaction and rotationally sampled turbulence. *Wind Energy* 2008; 11(4): 305–317. doi: 10.1002/we.249

8. Lackner MA, Rotea MA. Passive structural control of offshore wind turbines. *Wind energy* 2011; 14(3): 373–388.

9. Fitzgerald B, Basu B, Nielsen SRK. Active tuned mass dampers for control of in-plane vibrations of wind turbine blades. *Structural Control and Health Monitoring* 2013; 20(12): 1377–1396. doi: 10.1002/stc.1524

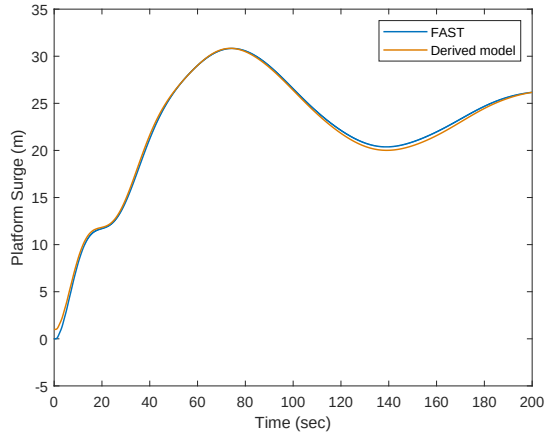

(a) Platform surge

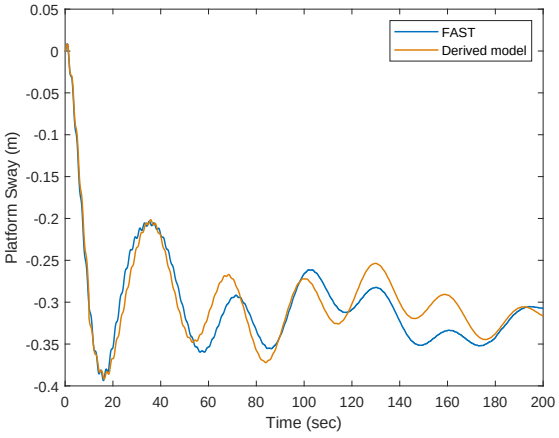

(b) Platform sway

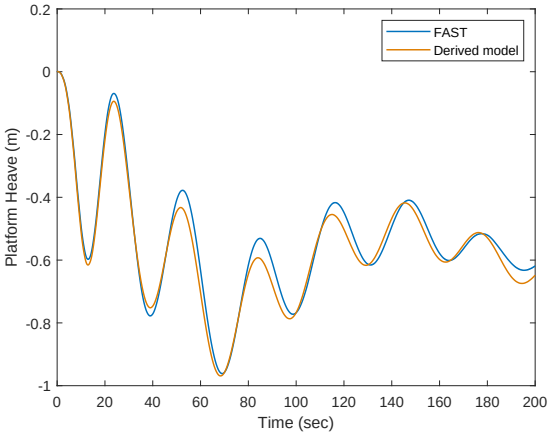

(c) Platform heave

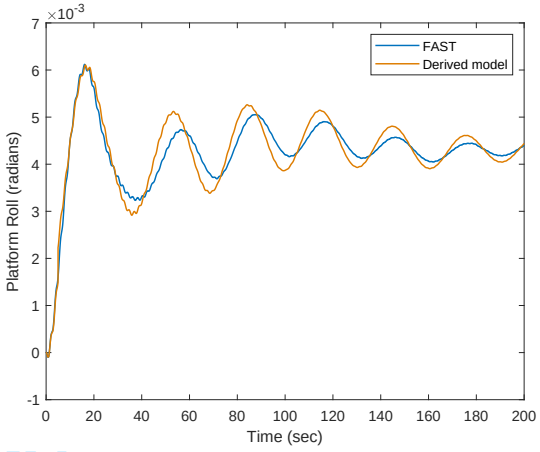

(d) Platform roll

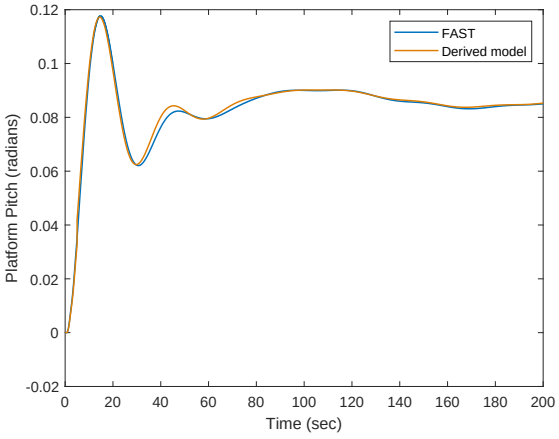

(e) Platform pitch

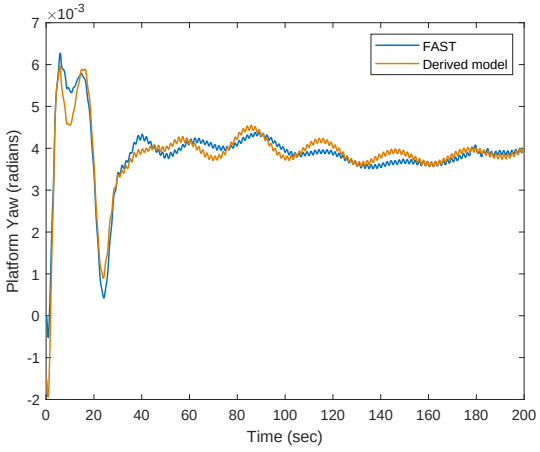

(f) Platform yaw

FIGURE B2 Model verification: motion of the wind turbine platform

10. Arrigan J, Pakrashi V, Basu B, Nagarajaiah S. Control of flapwise vibrations in wind turbine blades using semi-active tuned mass dampers. *Structural Control and Health Monitoring* 2011; 18(8): 840–851. doi: 10.1002/stc.404

11. Fitzgerald B, Arrigan J, Basu B. Damage detection in wind turbine blades using time-frequency analysis of vibration signals. In: IEEE. ; 2010: 1–5.

12. Lackner MA, Rotea MA. Structural control of floating wind turbines. *Mechatronics* 2011; 21(4): 704 - 719. doi: http://dx.doi.org/10.1016/j.mechatronics.2010.11.007

13. Fitzgerald B, Basu B. Structural control of wind turbines with soil structure interaction included. *Engineering Structures* 2016; 111: 131–151.

14. Fitzgerald B, Sarkar S, Staino A. Improved reliability of wind turbine towers with active tuned mass dampers (ATMDs). *Journal of Sound and Vibration* 2018; 419: 103–122.

15. Sarkar S, Chakraborty A. Optimal design of semiactive MR-TLCD for along-wind vibration control of horizontal axis wind turbine tower. *Structural Control and Health Monitoring* 2018; 25(2).

16. Sarkar S, Chakraborty A. Development of semi-active vibration control strategy for horizontal axis wind turbine tower using multiple magneto-rheological tuned liquid column dampers. *Journal of Sound and Vibration* 2019.

17. Ollgaard B, Jensen SP. Wind turbine tower having a damper. 2017. US Patent 9,657,717.

18. Jensen DK. Tuned liquid damper of a wind turbine. 2016. US Patent 9,234,505.

19. Smith MC. Synthesis of mechanical networks: the inerter. In: . 2. IEEE. ; 2002: 1657–1662.

20. Ikago K, Saito K, Inoue N. Seismic control of single-degree-of-freedom structure using tuned viscous mass damper. *Earthquake Engineering & Structural Dynamics* 2012; 41(3): 453–474.

21. Garrido H, Curadelli O, Ambrosini D. Improvement of tuned mass damper by using rotational inertia through tuned viscous mass damper. *Engineering Structures* 2013; 56: 2149–2153.

22. Marian L, Giaralis A. Optimal design of a novel tuned mass-damper-inerter (TMDI) passive vibration control configuration for stochastically support-excited structural systems. *Probabilistic Engineering Mechanics* 2014; 38: 156–164.

23. Lazar I, Neild S, Wagg D. Using an inerter-based device for structural vibration suppression. *Earthquake Engineering & Structural Dynamics* 2014; 43(8): 1129–1147.

24. Hu Y, Chen MZ. Performance evaluation for inerter-based dynamic vibration absorbers. *International Journal of Mechanical Sciences* 2015; 99: 297–307.

25. Hu Y, Wang J, Chen MZ, Li Z, Sun Y. Load mitigation for a barge-type floating offshore wind turbine via inerter-based passive structural control. *Engineering Structures* 2018; 177: 198–209.

26. Zhang R, Zhao Z, Dai K. Seismic response mitigation of a wind turbine tower using a tuned parallel inerter mass system. *Engineering Structures* 2019; 180: 29–39.

27. Ma R, Bi K, Hao H. Mitigation of heave response of semi-submersible platform (SSP) using tuned heave plate inerter (THPI). *Engineering Structures* 2018; 177: 357–373.

28. Kane TR, Levinson DA. *Dynamics, theory and applications*. McGraw Hill . 1985.

29. Jonkman JM, Buhl Jr ML. Fast user's guide-updated august 2005. tech. rep., National Renewable Energy Laboratory (NREL), Golden, CO.; 2005.

30. Jonkman BJ. TurbSim user's guide: Version 1.50. tech. rep., National Renewable Energy Lab.(NREL), Golden, CO (United States); 2009.

31. Burton T, Jenkins N, Sharpe D, Bossanyi E. *Wind energy handbook*. John Wiley & Sons . 2011.

32. Moriarty PJ, Hansen AC. AeroDyn theory manual. tech. rep., National Renewable Energy Lab., Golden, CO (US); 2005.

33. Hansen MO. *Aerodynamics of wind turbines*. Routledge . 2015.

34. Ning SA. A simple solution method for the blade element momentum equations with guaranteed convergence. *Wind Energy* 2014; 17(9): 1327–1345.

35. Ning A, Hayman G, Damiani R, Jonkman JM. Development and Validation of a New Blade Element Momentum Skewed-Wake Model within AeroDyn. In: ; 2015: 0215.

36. Dinh VN, Basu B. Impact of spar-nacelle-blade coupling on the edgewise response of floating offshore wind turbines. *Coupled Systems Mechanics* 2013; 2(3): 231-253.

37. MATLAB . *version 9.4.0 (R2018a)*. Natick, Massachusetts: The MathWorks Inc. . 2018.

38. Fitzgerald B, Staino A, Basu B. Wavelet-based individual blade pitch control for vibration control of wind turbine blades. *Structural Control and Health Monitoring* 2019; 26(1): e2284.

39. Fitzgerald B, Basu B. A monitoring system for wind turbines subjected to combined seismic and turbulent aerodynamic loads. *Struct Monit Maint* 2017; 4(2): 175–194.

40. Wendt FF, Robertson A, Jonkman JM, Hayman G. Verification of New Floating Capabilities in FAST v8. In: ; 2015: 1204.

41. Jonkman JM. *Definition of the Floating System for Phase IV of OC3*. Citeseer . 2010.

42. Giaralis A, Petrini F. Wind-induced vibration mitigation in tall buildings using the tuned mass-damper-inerter. *Journal of Structural Engineering* 2017; 143(9): 04017127.

43. Roberts JB, Spanos PD. *Random vibration and statistical linearization*. Courier Corporation . 2003.

44. Ditlevsen O. Stochastic model for joint wave and wind loads on offshore structures. *Structural Safety* 2002; 24(2-4): 139–163.

45. Stewart GM, Robertson A, Jonkman J, Lackner MA. The creation of a comprehensive metocean data set for offshore wind turbine simulations. *Wind Energy* 2016; 19(6): 1151–1159.

46. Murtagh P, Basu B, Broderick B. Along-wind response of a wind turbine tower with blade coupling subjected to rotationally sampled wind loading. *Engineering structures* 2005; 27(8): 1209–1219.